242–252 *Nucleic Acids Research, 2013, Vol. 41, No. 1* *Published online 3 November 2012*
doi:10.1093/nar/gks1028

Telomerase-dependent generation of 70-nt-long telomeric single-stranded 3′ overhangs in yeast

Helena Fridholm, Eimantas Astromskas and Marita Cohn*

Department of Biology, Genetics Group, Lund University, Lund, Sweden

Received June 13, 2012; Revised September 28, 2012; Accepted October 4, 2012

ABSTRACT

Telomeres, the chromatin structures at the ends of eukaryotic chromosomes, are essential for chromosome stability. The telomere terminates with a TG-rich 3′ overhang, which is bound by sequence-specific proteins that both protect the end and regulate the telomerase elongation process. Here, we demonstrate the presence of 3′ overhangs as long as 200 nt in asynchronously growing cells of the budding yeast *Saccharomyces castellii.* The 3′ overhangs show a wide distribution of 14–200 nt in length, thus resembling the distribution found in human cells. A substantially large fraction of the 3′ overhangs resides in the 70–200 nt range. Remarkably, we found an accumulation of a distinct class of 70-nt-long 3′ overhangs in the S phase of the cell cycle. Cells without a functional telomerase showed the same wide distribution of 3′ overhangs, but significantly, lacked the specific fraction of 70-nt 3′ overhangs. Hence, our data show that the highly defined 70-nt 3′ overhangs are generated by a telomerase-dependent mechanism, which is uncoupled to the mechanisms producing the bulk of the 3′ overhangs. These data provide new insights that will be helpful for deciphering the complex interplay between the specialized telomere replication machinery and the conventional DNA replication.

INTRODUCTION

Telomeres are essential for maintaining the stability of eukaryotic genomes. The telomere chromatin assembles into a protective cap structure that prevents the detection of the DNA ends by the DNA repair mechanisms, a process which could otherwise lead to illegitimate recombinations and end-to-end chromosome fusions. The chromatin assembly is driven by telomere proteins that associate with the tandemly repeated telomeric DNA with a high sequence specificity. Canonical telomere DNA structures consist of a highly TG-rich DNA strand running in the 5′ to 3′ direction towards the end of the chromosome and terminate in a single-stranded 3′ overhang protruding beyond the complementary CA-rich strand (1–3). The 3′ overhangs are the substrates for the telomerase, an enzyme that synthesizes the telomeric repeats by annealing to and extending the DNA 3′-end. Telomerase thereby counteracts the telomere erosion that stems from incomplete chromosome end replication by the conventional DNA replication machinery.

By establishing a balance of telomerase-mediated elongation and incomplete end replication, cells are able to maintain a constant average telomere length. The recruitment of telomerase is believed to be regulated by a switch between telomerase-extendable and telomerase–non-extendable states of the telomere chromatin (4). As the telomeric DNA progressively shortens in every cell division cycle, the chromatin structure is predicted to become less extensive and thereby less repressive. This would explain the observed preference of telomerase for short telomeres, and the fact that only a fraction of the telomeres is elongated in each cell cycle (5,6). However, the recruitment of telomerase is believed to be further regulated, as several proteins have been demonstrated to affect telomerase elongation, including known DNA-damage response factors. In budding yeast, Cdc13 plays a role in the recruitment of telomerase to the 3′-end through an interaction with the Est1 subunit of the telomerase holoenzyme. This process is regulated by a phosphorylation of Cdc13 by the Tel1 and Cdk1 kinases (7–9). Hence, as the 3′ overhangs are bound by specific proteins, which both positively and negatively regulate telomerase elongation, it is anticipated that a proper regulation of 3′ overhang generation is important for telomere function.

The elucidation of the separate parts of the telomere replication and how it is coordinated with the conventional replication machinery may provide insights into the process whereby cancer cells override the otherwise normal inhibition of the telomere lengthening, and may unravel targets for the development of new and efficient therapeutic strategies for cancer treatment. According to current general assumptions, the semi-conservative DNA replication of linear chromosomes leads to the generation of structurally distinct DNA termini (10). After the

*To whom correspondence should be addressed. Tel: +46 46 2227256; Fax: +46 46 2224113; Email: marita.cohn@biol.lu.se

removal of the RNA primer, the terminus generated by the lagging-strand synthesis will exhibit a short single-stranded 3′ overhang, whereas a blunt DNA end would be expected at the leading-strand end. However, it has been shown that both chromosome ends do indeed contain 3′ overhangs (2,3,11). Consequently, the blunt leading-strand telomeres need to be processed to generate the 3′ overhangs. The molecular mechanism of this processing is still unknown, but a trimming mechanism involving an exonucleolytic cleavage of the CA-rich strand has been proposed, a so-called 5′ resection. Surprisingly, even though telomeres should be avoided by the double-strand break repair pathway, telomeres and double-strand breaks seem to be resected by similar machineries (12). Furthermore, the finding that the terminal repeat sequence of the CA-rich strand in mammalian cells usually ends with the same permutation indicates that the resection is regulated (13). Accordingly, the ciliate *Euplotes crassus* has short highly regulated 14-nt 3′ overhangs, which are bound by a single telomere end-binding protein (14). In contrast, the 3′ overhangs in human cells can be several hundred nucleotides in length and are correlated with the presence of several molecules of the single-stranded telomeric DNA-binding protein Pot1 (15,16). In *Saccharomyces cerevisiae*, the 3′ overhangs have been reported to be 12–14 nt in most parts of the cell cycle (17). However, transiently elongated 3′ overhangs (>30 nt) were detected in late S phase, which is the time point when telomerase acts at the telomere (1,18). Interestingly, the timing of the lengthening is also correlated with an enrichment of Cdc13 at the telomeres (17,19).

The budding yeast *Saccharomyces castellii* (synonym of *Naumovozyma castellii*) is phylogenetically located in a clade branching off after the whole-genome duplication event that took place in the *Saccharomyces* lineage, and it has a genome size of 9.7 Mb divided on 10 chromosomes (20,21). We have previously shown that *S. castellii* is amenable for molecular genetic manipulation, such as transformation and gene disruption, and that commonly used *S. cerevisiae* resistance markers are functional in *S. castellii* (22,23). Because of the high repeat addition processivity in the *in vitro* telomerase assays, *S. castellii* provides an ideal model organism for the study of the molecular mechanisms of telomere maintenance (24). The homogeneous 8-nt telomere repeats (TCTGGGTG) in *S. castellii* have enabled the precise determination of the minimal binding sites for the Rap1 and Cdc13 homologues on the respective double- versus single-stranded telomeric DNA (25–28). Furthermore, the finding that Rap1 and Cdc13 are dependent on coinciding nucleotide positions within the *S. castellii* telomere repeat sequence, and that these positions are highly conserved in evolution, led to the conclusion that they act together to preserve a core sequence of the telomeric DNA (29).

In this work, we aimed to study the telomeric 3′ overhangs in *S. castellii* cells. To that end, we modified the assay based on the digestion with duplex-specific nuclease (DSN) (16). In the DSN assay, the double-stranded genomic DNA is cut into <10 bp fragments by the DSN enzyme, whereas the single-stranded 3′ overhangs are left intact, thus enabling the detection of the full range of the 3′ overhang lengths by Southern blot hybridization. We demonstrate that the 3′ overhangs have a remarkably wide length span, with an abundant 70–200 nt fraction detectable in unsynchronized *S. castellii* cells. Remarkably, we found a fraction of 3′ overhangs with a defined length of ~70 nt, which is dependent on an active telomerase enzyme for its generation in the S phase of the cell cycle. Thus, we were able to identify and monitor a distinct process for the generation of 3′ overhangs, which will be highly valuable for the possibility to distinguish separate activities within the telomere replication mechanism.

MATERIALS AND METHODS

Yeast strains

The *S. castellii* strains used in this study were Y320 (*MAT*α, *ura3*, *ho*); Y235 (*MAT*a/*MAT*α, *ura3*/*ura3*) (22,23); NRRL Y-12630 (type strain), YMC121 and YMC124 (*MAT*a/*MAT*α, *ura3*/*ura3*, *tlc1::KanMX*/*tlc1::KanMX*); YMC122 and YMC123 (*MAT*a/*MAT*α, *ura3*/*ura3*, $TLC1^{+}/TLC1^{+}$) (23).

Bal31 assay

Saccharomyces castellii Y320 genomic DNA (1 μg) was incubated together with 5 U of Bal31 nuclease (New England Biolabs) for increasing time, and reactions were stopped by adding EGTA to a final concentration of 33 mM. The DNA was subsequently diluted with the appropriate buffer and was digested with PstI for 1 h. After electrophoresis in 0.8% agarose gel [1× TBE buffer: 89 mM of Tris–borate and 2 mM of ethylenetetraaceticacid (EDTA)], the DNA was transferred to a Hybond-N^{+} nylon membrane (Amersham). The oligonucleotide probe Scast16B (5′-TGTCTGGGTGTCTGGG) was labelled in the 5′-end with T4 polynucleotide kinase (New England Biolabs) and γ-^{32}P-adenosine triphosphate. Hybridization was performed at 40°C overnight [0.25 M of Na_2HPO_4, 7% of sodium dodecyl sulphate (SDS), 1 mM of EDTA]. The membrane was washed twice for 10 min at room temperature in 100 mM of Na_2HPO_4 and 2% of SDS. Signals were visualized with the phosphorimager Molecular Imager® FX (Bio-Rad).

In-gel hybridization

Genomic DNA was extracted from *S. castellii* Y320 as described in (30) with the following modifications: the spheroplasts were incubated with proteinase K in EDS buffer (50 mM of EDTA, 0.2% of SDS) for 1 h at 37°C; 5 M ammonium acetate was used in the DNA precipitation steps. The genomic DNA, 6 μg, was cleaved with PstI and resolved in 0.8% agarose gel in 1× TBE buffer. The gel was hybridized overnight at room temperature using the 5′ labelled oligonucleotide (5′-ACCCAGACACCCAG ACACC) or (5′-TGTCTGGGTGTCTGGG), using a modified hybridization buffer (5 × SSC, 5 × Denhardts solution, 20 μg/ml denaturated salmon sperm DNA) as previously described (31). Gels were washed twice for 1 h at room temperature and once at 30°C for 1 h with 0.25 × SSC. Signals were quantified using the Quantity

One software (Bio-Rad). To correct for loading differences, the signal intensities obtained from the native gel were divided by the signal obtained from the ethidium bromide stained gel. As a control for the native conditions, a linearized plasmid with a telomere sequence insert was either untreated or denatured by boiling for 2 min before loading. After collecting the 3′ overhang signals, the gel was denatured, neutralized and re-hybridized as aforementioned to obtain the terminal restriction fragment (TRF) patterns.

Synchronization of *S. castellii*

Saccharomyces castellii Y320 was grown in YPD medium (1% yeast extract, 2% peptone, 2% D-glucose) at 25°C. At optical density (OD_{600}) ~0.5, cells were arrested in early S phase by addition of 150 mM *N*-hydroxyurea (AppliChem). After a 4 h incubation at 25°C, >95% of the cells displayed a dumb-bell shape. The cells were washed in and released in pre-warmed YPD. Samples were collected every 10 min, pelleted and resuspended in ice cold 15% glycerol in 1 × TNE (1 mM of Tris–HCl pH 7.4, 10 mM of NaCl, 0.1 mM of EDTA) and stored at −20°C until used for the DNA preparation.

Flow cytometry

Harvested yeast cells were resuspended in 300 µl of water and were fixed by dropwise addition of 700 µl 95% ethanol and were incubated at 4°C overnight. The fixed cells were pelleted, resuspended in 50 mM of citrate buffer pH 7.4 and sonicated for 10 s (setting 30%, 1 s pulses). Treatment with 0.25 mg/ml RNase A at 50°C for 2 h, and with 1 mg/ml proteinase K at 50°C for 2.5 h, was followed by staining in 16 µg/ml propidium iodide in 50 mM citrate buffer pH 7.4. Flow cytometry analysis was performed on a BD Accuri C6 Flow Cytometer equipped with a CSampler (BD Biosciences), and data were collected in the CFLow Sampler software.

DSN assay of single-stranded 3′ overhangs

Genomic DNA was isolated with the Promega Wizard® Genomic DNA Purification Kit, and 2.5 µg was digested with 0.5–1 U of duplex-specific nuclease (DSN; Evrogen) for 3 h at 37°C. The specificity of DSN to double-stranded DNA was tested on genomic yeast DNA, λDNA and *S. castellii* telomeric DNA, and it did not digest single-stranded DNA. The sporulated telomerase knock-outs were dissected and grown to colonies. After re-streaking on new plates, the resulting colonies were used to inoculate liquid cultures that were grown overnight (representing a total of >60 cell generations before DNA preparation). A pre-treatment with the 3′–5′ exonuclease I (New England Biolabs, ExoI) was used as a control for the reduction of 3′ overhangs. DNA was digested with 30 U of ExoI in DSN buffer for 2 h at 37°C before the DSN cleavage. Equal volume of deionized formamide was added, and samples were boiled 2 min before loading on 10% polyacrylamide gels at denaturing conditions (8 M of urea) in 0.5 × TBE buffer. Molecular size markers: telomeric sequence oligonucleotides (12, 19, 39 and 71 nt) and 5′-end-labelled GeneRuler SM1211 (Fermentas). Electrotransfer was performed in 0.5 × TBE with the settings of 25 V (constant), 300 W and 3.5 mA/cm^2 for 5 min in a semi-dry blotter (BioRad semidry transfer cell) onto a nylon membrane (porablot NY plus, Macherey-Nagel), with subsequent ultraviolet-cross-linking (Spectrolinker^{TM} XL-1000 UV Crosslinker). Pre-hybridization was performed for a minimum of 2 h in 0.25 M of Na_2HPO_4, 7% of SDS and 1 mM of EDTA at 35°C before the addition of the α-^{32}P-dCTP-labelled probe (5′-ATT CAG ACA CCC AGA CAC CC-3′), and hybridization was performed at 35°C overnight. The membrane was washed twice at room temperature for 5 min and twice at 35°C for 15 min in 100 mM of Na_2HPO_4 and 2% of SDS, followed by a quick rinse in 2 × SSC. Signals were visualized and analysed with a phosphorimager. The membranes were not analysed below the 19-nt marker, as the stringency used markedly reduced the signal of a 12mer marker. Quantifications of radioactive signals were performed by collecting data from similarly sized areas of all samples, with background signal reduction. Normalization of hybridization signals were performed by dividing the signals from similarly sized windows at 20, 40, 60, 75, 100 and 200 nt, with the factor corresponding to the multiples of the 20-nt probe length (40/2, 60/3, 75/3.75, 100/5 and 200/10). For analyses of larger size fractions, the lane was divided into windows, denoted short (S) 20–40 nt, medium (M) 40–60 nt, long (L) 60–90 nt and ultra-long (UL) 90–200 nt.

RESULTS

Telomeric 3′ overhangs are clearly detectable in unsynchronized *S. castellii* cells

Telomeric 3′ overhangs are required for the formation of the protective telomere structure and also provide the substrate for telomerase elongation. However, there are several aspects of the 3′ overhang generation that remain poorly understood. To explore the possibility of detecting single-stranded 3′ overhangs in *S. castellii*, we initially developed the TRF analysis for *S. castellii* genomic DNA and performed the conventional in-gel hybridization. The telomeres were released by a restriction enzyme cleaving in the subtelomeric region, and they were visualized by Southern blot hybridization with a telomeric probe (Figure 1). Telomeric fragments display a smeary appearance in Southern blots because of the cellular variation in length. Moreover, the terminal positioning of a fragment is assessed by the disappearance of the band after digestion of the genomic DNA with the Bal31 exonuclease. We found that PstI produced bands of a suitable size for analysis, which were highly sensitive to Bal31 treatment (Figure 1). By using the decrease in size of the smallest band, we calculated the telomere tract length to ~250 bp (with a size distribution of ±180 bp in the fuzzy band). This seems to be the size of the majority of the telomeres, as most of the bands are digested by Bal31 with the same rate. Thus, the telomere length in *S. castellii* is similar to that found in *S. cerevisiae*.

Next, we analysed the single-stranded telomeric 3′ overhangs of *S. castellii* by performing in-gel hybridizations

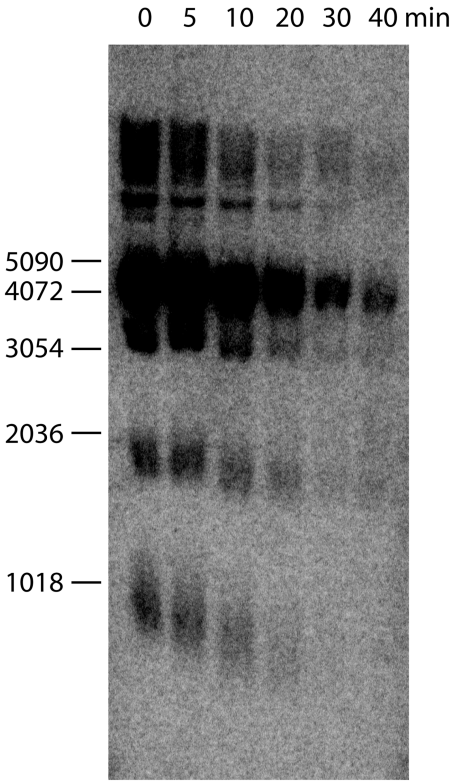

Figure 1. TRF analysis and Bal31 assay of *S. castellii* telomeres. *S. castellii* genomic DNA was treated with Bal31 exonuclease for increasing periods and was then cleaved with PstI. The DNA was separated on an agarose gel, and the Southern blot membrane was hybridized with a telomeric probe to detect the TRFs containing the telomeres. Top: Bal31 digestion time indicated in minutes. Left margin: molecular size marker indicated in bp.

under native conditions. TRFs were released and separated in an agarose gel as in the TRF analysis aforementioned, and in-gel hybridization was performed with telomeric repeat probes directed towards the TG- or CA-rich strands (Figure 2). With the probe for the TG-rich strand, we obtained easily detectable signals (Figure 2A, native gel, lane 1), whereas the probe for the CA-rich strand did not give any signals above the background (Figure 2B, native gel, lane 1). A plasmid containing *S. castellii* telomeric repeats was used as a control of the experimental conditions. The non-denaturated linearized plasmid did not show any signal in the native gel, thus confirming the non-denaturing conditions of the experiment (Figure 2A and B, native gel, lane 3). In contrast, the plasmid that was denatured before loading showed hybridization signals in the native gels (Figure 2A and B, native gel, lane 4). Subsequently, the gels were denatured and re-hybridized with the respective probes for the TG- and CA-rich strands. The banding pattern obtained after denaturation was similar to the native gel, which corresponded to the TRF banding pattern, and thus verified the presence of double-stranded telomeric sequences. To additionally confirm that the signals in the native gels correspond to the 3′ overhangs, we pre-treated the genomic DNA with exonuclease I (ExoI), which specifically removes single-stranded DNA from the 3′ terminus. As expected, the ExoI treatment clearly reduced the signal in the native gel, but did not affect the signals in the denatured gel (Figure 2A, lane 2). Thus, in contrast to the situation in *S. cerevisiae* where signals are only detected when cells are synchronized in S phase (1), the 3′ overhangs in *S. castellii* give clearly detectable signals in the in-gel hybridization of DNA prepared from non-synchronically growing cells.

Detection of telomeric 3′ overhangs in synchronously growing cells

Next, we wanted to investigate whether the single-stranded 3′ overhang signals would be detectable in separate phases of the cell cycle. A synchronization protocol for *S. castellii* was developed based on *N*-hydroxyurea, which is known to arrest *S. cerevisiae* in the early stages of the S phase (32). Incubation of *S. castellii* cells for 4 h in 150 mM hydroxyurea resulted in 95% of cells having the characteristic dumb-bell shape (as compared with 87% of the *S. cerevisiae* cells used as a control) (Supplementary Figure S1A). The efficient cell cycle block in early S phase was further confirmed by flow cytometry analysis of propidium iodide stained cells (Figure 3A). The cells were released from the cell cycle block by washing and resuspension in fresh YPD medium, and the synchronous growth was verified by flow cytometry analysis (Supplementary Figure S1B). The cells were observed to progress through S phase and to accumulate in the G2 phase. Finally, the cells started to enter the G1 phase. Furthermore, the treated cells showed the same viability count as untreated cells when spread on YPD plates. Thus, an efficient cell cycle block was obtained in *S. castellii* after 4 h incubation in 150 mM of hydroxyurea. This block was readily reversible after the removal of the drug, and the cells progressed in synchrony through the S phase and G2 phase.

To investigate the single-stranded 3′ overhangs in the cell cycle, synchronized *S. castellii* cells were released into S phase, and samples for DNA preparation were taken every 10 min. The time course experiment was performed for 110 min. Genomic DNA was extracted and analysed by native in-gel hybridization, and the 3′ overhang signals were quantified (Figure 3B). The result showed that the 3′ overhang signals were readily detectable during the full experimental time course, and that it did not exhibit any drastic variations. Nonetheless, a minor peak was observed at 30 min after release. Thus, we obtained readily detectable signals for telomeric single-stranded 3′ overhangs throughout the S phase and the G2 phase of the cell cycle.

A distribution of 14- to 200-nt-long 3′ overhangs in unsynchronized cells

The global signal obtained in the in-gel hybridization method does not provide any information on the actual lengths of the telomeric 3′ overhangs. Therefore, we developed the DSN assay for the examination of 3′ overhang lengths in yeast cells (16). Total genomic DNA from unsynchronized *S. castellii* Y320 and Y12630 cells was digested with the DSN, which cleaves the

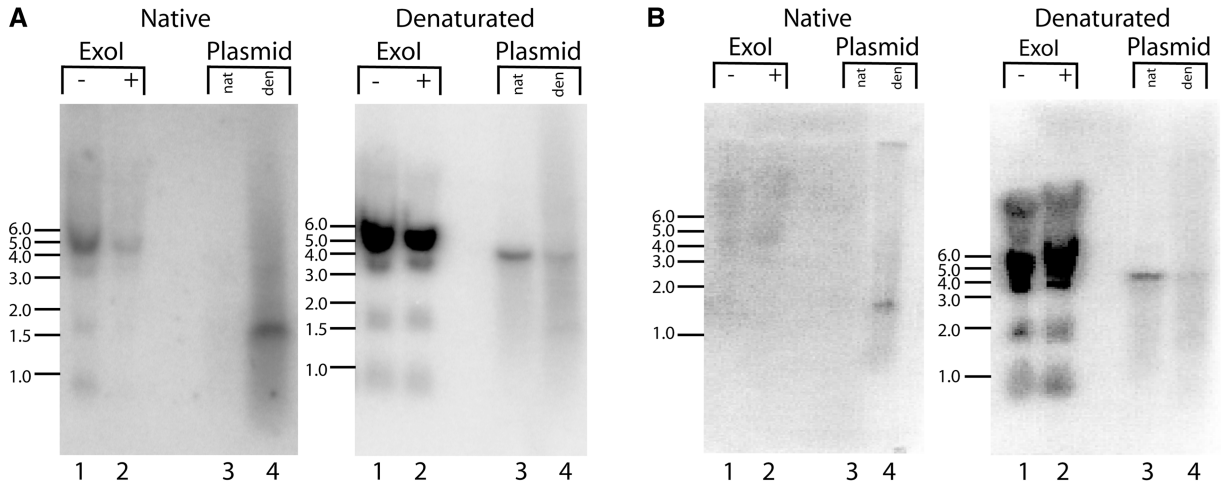

Figure 2. Detection of *S. castellii* telomeric single-stranded 3′ overhangs by in-gel hybridization. Genomic DNA was cleaved with PstI and was separated on an agarose gel, and the in-gel hybridization was performed with a telomeric probe at native conditions. After exposing the native gel, it was denatured and rehybridized with the same probe to detect the total telomeric DNA. Lane 2, treatment of the genomic DNA with exonuclease I (ExoI) before PstI cleavage. Plasmids containing *S. castellii* telomeric sequences were used as a control for the native gel conditions, native plasmid (lane 3) and denaturated plasmid (lane 4). (**A**) Hybridization with the probe annealing to the TG-rich strand. (**B**) Hybridization with the probe annealing to the CA-rich strand.

double-stranded DNA to <10 bp fragments while leaving the single-stranded 3′ overhangs intact. The 3′ overhangs were separated by denaturing polyacrylamide gel electrophoresis and were visualized by Southern blot hybridization with a telomeric probe (Figure 4A). The DSN assay revealed a smeary hybridization pattern, with a surprisingly wide size-span ranging from ~20 to more than ~300 nt in length (Figure 4A). To verify the 3′ overhangs, a parallel sample of genomic DNA was pre-treated with the ExoI exonuclease before proceeding with the DSN assay. Remarkably, the ExoI pre-treatment abolished the signal in a span from ~20 to ~200 nt (Figure 4A). It should be noted that because of the stringency of the hybridization, we are not able to analyse the gels below the 19-nt marker. Moreover, the DSN enzyme leaves 5–6 bp of undigested double-stranded DNA at the junction of the double-stranded and single-stranded DNA (16). Thus, the signal at 20 nt corresponds to a single-stranded 3′ overhang with a minimum length of ~14 nt. As an additional control, genomic DNA was pre-treated with the T7 exonuclease, a 5′–3′ exonuclease, which will create longer 3′ overhangs on DNA ends. Pre-treatment of the genomic DNA with T7 exonuclease increased the signal of the smear in the full 20–200 nt range, thus confirming that the detected signals are 3′ overhangs (Supplementary Figure S2).

Because longer overhangs will be annealed to a larger number of probe molecules in the hybridization, the actual output signal will not indicate the proper relative abundance of the different 3′ overhang lengths. Therefore, we normalized the signals of selected size fractions to the number of 20-nt-probe molecules that would anneal to the respective overhang lengths. Similarly sized quantification windows at 20, 40, 60, 75, 100 and 200 nt were selected, and the signals were divided with the respective 20-nt size factor (40/2, 60/3, 75/3.75, 100/5 and 200/10). The normalized values retrieved from these analyses were used to calculate the ratio of each size window to the total of all windows. This analysis revealed that the large overhang sizes (75–100–200 nt) still give values comparable with the other size groups, despite of the reduction of the signals in the normalization procedure (Figure 4B). When analysing four samples grown at separate time points and in different conditions, a mean value of 60% was retrieved for the sum of the 75–100–200 nt sizes (Figure 4B). Even though the distribution varied in between experiments, they uniformly showed a high proportion of 3′ overhangs of a size ≥75 nt (ranging from 33 to 80%).

To summarize, these results show that within a population of non-synchronously growing yeast cells, there is a remarkably wide distribution of 3′ overhang lengths, ranging from short, 14 nt, to unexpectedly long, 200 nt, 3′ overhangs. Although the distribution of 3′ overhang lengths is dynamic in the full range of 14–200 nt, with different cultures giving a slightly different size distribution, a surprisingly large fraction of the 3′ overhangs is within the 75–200 nt range.

A distinct fraction of 70-nt-long 3′ overhangs

When performing the DSN assay on DNA samples from cultures grown at various conditions, we observed a distinct and relatively strong signal occurring at the size of ~75 nt in some of the cultures (Figure 5). This striking and prominent band showed a clear sensitivity to ExoI (Figure 5). A subtraction of the 5–6 nt left at the double- and single-stranded junction by DSN gives a size of ~69–70 nt for the 3′ overhangs within this distinct band. We will, therefore, refer to this band as the 70-nt 3′ overhangs. Despite the stochastic variance between cultures, the appearance and relative signal intensity of the 70-nt 3′ overhangs was reproducible for separate DSN assays made of the same DNA preparation. Furthermore, the distinct band was detected in three different *S. castellii* strains; Y320, Y235 and NRRL Y-12630 (type strain)

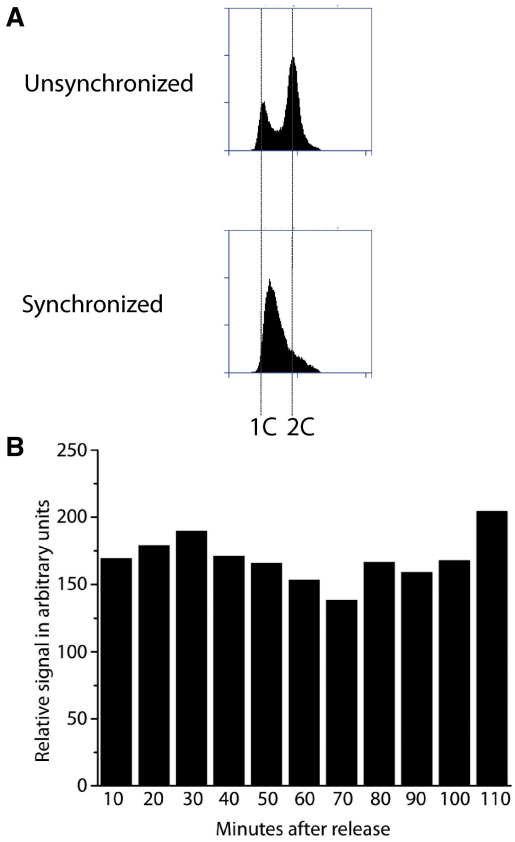

Figure 3. Detection of telomeric 3′ overhangs in synchronized *S. castellii* cells. (**A**) Flow cytometry analysis of propidium iodide stained *S. castellii* cells. Cells treated with *N*-hydroxyurea were efficiently blocked in S phase (synchronized), whereas untreated cells (unsynchronized) showed a distribution between all phases of the cell division cycle. The positions indicated by 1C and 2C denote cellular DNA content and represent the signals from the cells in G1 and G2, respectively. (**B**) Synchronized cells were released into S phase, and samples for DNA preparation were withdrawn every 10 min. The telomeric 3′ overhangs were analysed by native in-gel hybridization, and the signals were quantified. The bars represent the total 3′ overhang signals (in arbitrary units) for the respective time points after release. All signals are normalized for the total DNA loading.

(Figure 5 and data not shown). However, the abundance of the 70-nt overhangs varied between cultures grown at different occasions, and we observed that the presence of the 70-nt 3′ overhangs was correlated with a high cell density of the culture. The signal could be detected in cultures of $OD_{600} \geq 0.7$, whereas it was not detected in cultures with $OD_{600} \leq 0.5$. Possibly, this could be caused by oscillations of the cell culture, a phenomenon occurring at high cell densities, which leads to partial synchronization of the cells (33).

Cell cycle regulated dynamics of the 3′ overhangs

To investigate whether any cell cycle-dependent changes would occur in the distribution of single-stranded 3′ overhangs, *S. castellii* cells were synchronized and released into S phase. Samples for the DSN assay were collected just before addition of the hydroxyurea, as well as at the time of release, and then at every 10 min (Figure 6 and Supplementary Figure S3). The unsynchronized cells showed the same smeary and wide distribution of 3′ overhangs as previously seen in our unsynchronized cells (Figure 6, denoted Pre). However, in the synchronized cells, a dramatic shift in the distribution was seen, where the fraction of 70-nt 3′ overhangs appeared strongly in relation to the other signals (Figure 6, denoted 0). Interestingly, the 70-nt 3′ overhangs gradually diminished in the subsequent time points, to eventually become almost undetectable. This dynamic behaviour of the 70-nt-3′ overhang signal was seen in four separate time course experiments, showing the same overall pattern with an accumulation of signal in the synchronized cells followed by a gradual decrease in the released and synchronously growing cells (Figure 6 and Supplementary Figure S3). This result indicates that the 70-nt 3′ overhangs are generated in the S phase and then gradually disappear as the cells proceed in the cell cycle.

Flow cytometry analysis of propidium iodide stained cells showed that the hydroxyurea stalls the cells in early S phase, and following release, the cells proceed in synchrony from S to G2 phase (Supplementary Figure S1B). However, even if we did not expect the cultures to stay synchronized after the passage of G2/M, we nonetheless continued the sampling for an extended period. Intriguingly, flow cytometry analyses of time course experiments lasting for 130 min revealed that a fraction of the cells proceeded in synchrony through the G2/M, G1 and S phases, to finally accumulate a second time in the G2 phase (Supplementary Figure S4). Thus, a minor fraction of the cells proceeded in synchrony for more than one full cell division cycle. Moreover, when analysing the 3′ overhangs of extended time course experiments, we made the intriguing observation that the signal of the 70-nt 3′ overhangs reoccurred in a periodical pattern throughout the experiment. The experiment shown in Figure 6 was performed for 300 min, and after the decrease seen in the first 10–60 min time points, the signal increases again and peaks at 110 min (Supplementary Figure S3A). However, surprisingly, it reappears at 200–250 min and then again at 300 min (Supplementary Figure S3A). In the other time course experiments performed, lasting for 120–140 min, this first reappearing signal was similarly observed (Supplementary Figure S3B). Notably, the reappearance of the 70-nt 3′ overhangs coincides with the timing of the new S phase of the minor fraction of the cells that proceed in synchrony through G2/S. This observation, together with our results showing that the 70-nt 3′ overhangs accumulate during the block in S phase and then decrease as the cells are released and entering G2, indicates that the 70-nt 3′ overhangs are specifically generated in the S phase.

Furthermore, we observed that the decrease in the 70-nt overhangs after release was not a result of merely a total decrease of 3′ overhangs, as some of the other overhang sizes were still present at similar amounts or even higher amounts. To facilitate the analyses and the discussion of the changes in the distribution of 3′ overhang signals, we divided each lane into four size windows; short 20–40 nt, medium 40–60 nt, long 60–90 nt and ultra-long 90–200 nt (Figure 6). Hence, in this grouping, the 70-nt 3′ overhangs belong to the long fraction. As aforementioned, the long

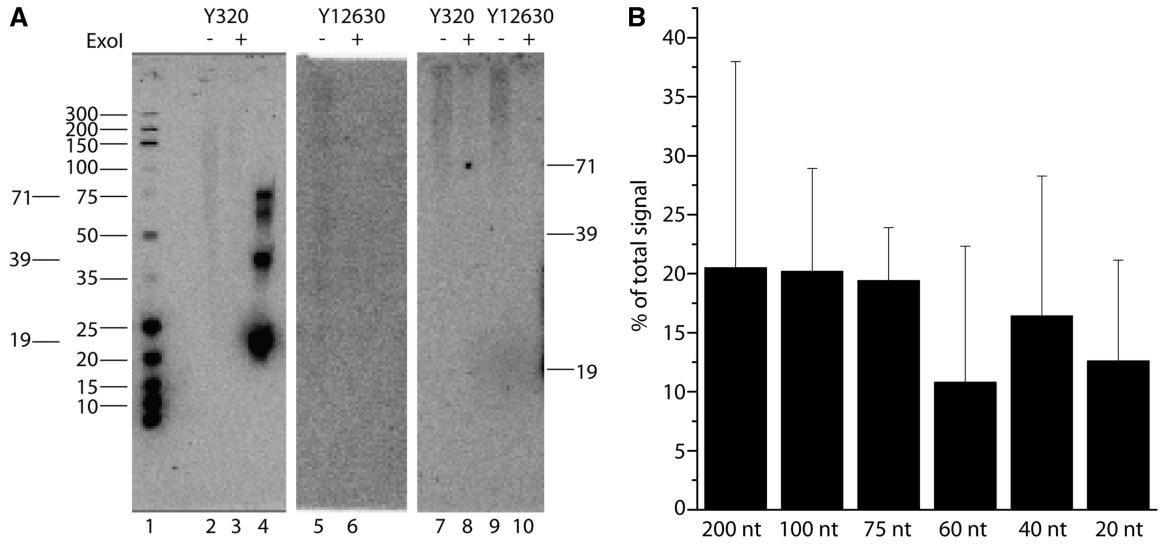

Figure 4. The telomeric 3′ overhangs in *S. castellii* exhibit a wide size distribution, ranging between 14–200 nt. (**A**) DSN assay of genomic DNA from unsynchronized *S. castellii* strains. ExoI + or − denotes with or without exonuclease I pre-treatment. Lanes 2–3, 2.5 μg Y320 DNA; lanes 5–6, 1.5 μg Y12630 DNA; lanes 7–10, 5 μg Y320 or Y12630 DNA. Molecular size markers are indicated in nucleotides: lane 1, GeneRuler molecular size marker; lane 4, telomere oligonucleotide markers. (**B**) A large proportion of the 3′ overhangs (60%) are within the 75–200 nt size fraction in unsynchronized *S. castellii* Y320 cells. The signals in selected size windows (200, 100, 75, 60, 40 and 20 nt) of the DSN assays were quantified. The bars indicate the percentages of each size within the total signal of all sizes. Mean values of four separate experiments are shown.

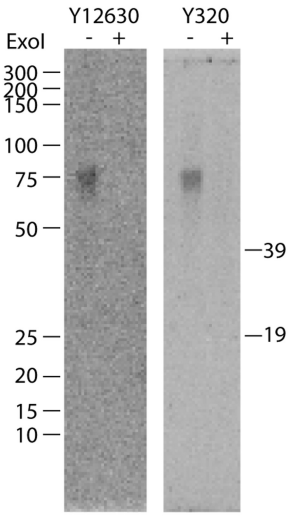

Figure 5. A distinct class of 70-nt-long 3′ overhangs shows a high abundance in unsynchronized cells. DSN assays were performed on genomic DNA from unsynchronized cultures of *S. castellii* strains Y12630 and Y320 grown to a high OD_{600}. The 70-nt 3′ overhangs show a predominant signal, which is abolished by pre-treatment with exonuclease I. Size markers are indicated in nucleotides.

signal is lacking in the unsynchronized sample but is predominant at the 0 min time point of the synchronized cells (Figure 6, Pre versus 0). On the other hand, the ultra-long fraction shows a contrary pattern, showing a predominance in the unsynchronized sample (Pre), but a decreased level at the 0 min time point. We observed this contrary distribution for the ultra-long and long signals in several of the time points, but it is, however, not a clear trend throughout the whole time course. Instead, we note that the signal distribution is fluctuating. Thus, in contrast to the long fraction, the signals from the ultra-long, medium and short fractions seem to undergo stochastic changes throughout the time course, and quantification of the fractions did not give any coherent pattern between the separate experiments.

In summary, we observed a dynamic length distribution of the 3′ overhangs during the progression of the cell cycle, including changes in the full range of 14–200 nt sizes. Most prominently, the highly defined fraction of 70-nt 3′ overhangs was found to be generated in the S phase.

The formation of the 70-nt-long 3′ overhangs is telomerase-dependent

Telomeric single-stranded 3′ overhangs could be generated either by telomerase extension of the TG-rich strand or by a resection of the complementary CA-rich strand by an exonuclease. Previous reports have shown that the telomerase extension activity is not necessary for the generation of 3′ overhangs per se (31). However, as we observed such a wide distribution of 3′ overhang lengths, we were interested to know whether telomerase would be involved in the generation of a certain size fraction of the 3′ overhangs. To this end, we analysed *S. castellii* cells where the gene encoding the telomerase RNA component (*TLC1*) was disrupted and thus lacked telomerase activity (23). The telomerase knock-out was performed in the diploid strain Y235, which was subsequently sporulated, and the spores were separated by micro-dissection. The respective wild-type and knock-out spores from two separate sporulation tetrads were analysed by the DSN assay (Figure 7A and data not shown). In the wild-type strains, we observed a similar smeary pattern of 3′ overhangs as previously seen, ranging from 14 to 200 nt, and with a marked signal of the 70-nt overhangs (Figure 7A). Also in the telomerase knock-out cells, 3′ overhangs in the full 14–200 nt range could be detected. Surprisingly, the defined 70-nt-

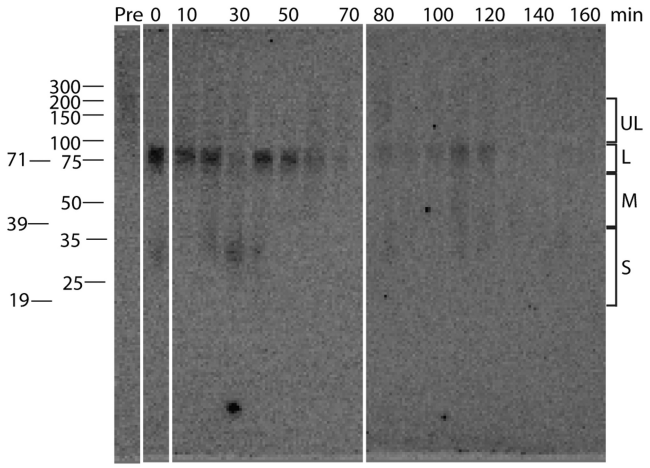

Figure 6. The fraction of 70 nt 3′ overhangs are generated in S phase. *S. castellii* Y320 cells were synchronized by hydroxyurea treatment and released into S phase. Samples for DNA preparation and DSN assay were collected just before addition of the hydroxyurea (Pre), at the time of release from the hydroxyurea block (0), and then at every 10 min. Size markers are indicated in nucleotides. The lower signal at the 30 min time point is because of loss of material during loading. The size windows used for quantification of the signals are indicated to the right; S, short 20–40 nt; M, medium 40–60 nt; L, long 60–90 nt; UL, ultra-long 90–200 nt. The full time course of 300 min is shown in Supplementary Figure S3A.

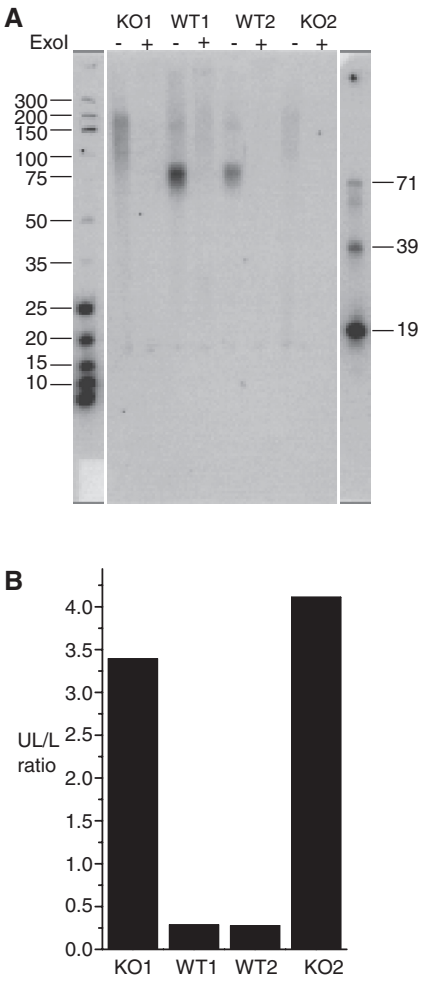

Figure 7. The 70-nt 3′ overhangs are generated by a telomerase-dependent mechanism. Knock-out of the *TLC1* gene was performed in the diploid *S. castellii* Y235 strain, the transformants were sporulated and the four separate spore products in a tetrad were analysed by the DSN assay. WT1 and WT2, $TLC1^{+}$ wild-type spores; KO1 and KO2, $tlc1^{-}$ telomerase knock-out mutants. (**A**) Telomerase knock-out mutants did not show any signals of the 70-nt 3′ overhangs. With or without pre-treatment with exonuclease I is indicated with + and −. Size markers are indicated in nucleotides. (**B**) Telomerase knock-out mutants show a higher ratio of ultra-long to long signals (UL/L) in the DSN assay. The signals of the 3′ overhangs belonging to the respective ultra-long (UL; 90–200 nt) and long (L; 60–90 nt) size windows were quantified in the gel shown in (A), and the UL/L ratio was calculated within the respective lanes.

overhang signal was lacking in the telomerase knock-out cells (Figure 7A). A quantification analysis of the relative distribution of the signal in the respective lane showed that the wild-type samples have a four times higher percentage of the signal in the long window (includes the 70-nt fragments) as compared with the knock-out cells (Table 1). In contrast, the fraction of the ultra-long signal is three times lower for the wild-type cells compared with the knock-out cells (Table 1). To quantitatively determine the relationship between the ultra-long (UL) and long (L) 3′ overhangs, the ratio of UL/L signals was calculated within each sample (Figure 7B). This showed a clear difference in the UL/L ratios between wild-type and knock-out cells, indicating distinct differences in the distribution of 3′ overhangs within these size fractions.

In conclusion, we have shown that yeast cells exhibit a wide distribution of 3′ overhang lengths, ranging between 14 and 200 nt, and that the distribution of sizes changes dynamically during the progression of the cell cycle. As the full range of 14–200-nt-long 3′ overhangs are present in telomerase negative cells, the majority of the 3′ overhangs are probably generated by telomerase-independent mechanisms, including the gap left by the conventional replication of the lagging strand as well as a 5′-resection of the CA-rich strand. Strikingly, we found that a fraction of 3′ overhangs with a defined length of 70 nt is generated in the S phase of the cell cycle, and the generation of these 70-nt 3′ overhangs is dependent on an active telomerase enzyme.

DISCUSSION

Telomeres confer genome stability by preventing the recognition of the DNA ends by the DNA repair mechanisms and protecting the ends from degradation by cellular nucleases. The single-stranded 3′ overhangs are ubiquitous structures of eukaryotic telomeres and play critical roles in the end protection. Moreover, they provide the potential for telomere homeostasis by serving as the substrates for extension by telomerase. Although the genetic requirements for telomere protection and elongation have been extensively studied in many organisms, the mechanism for 3′ overhang generation is still unclear, and the nucleases responsible for the controlled processing of the telomere ends remain unidentified. In this study, we investigated the single-stranded telomeric 3′ overhangs in the budding yeast *S. castellii*, which has TG-rich and highly homogeneous 8mer telomeric repeats (TCTGGGTG) (25).

Table 1. Relative distribution of 3′ overhang sizes (%)

3′overhang size window	Number of nucleotides	WT1	WT2	KO1	KO2
Ultra-long	90–200	21	21	63	68
Long	60–90	72	76	19	16
Medium	40–60	5	2	10	8
Short	20–40	2	0	8	8

Relative distribution of 3′ overhang sizes within the telomerase knock-out cells (KO) and wild-type cells (WT) assayed in Figure 7A. The indicated size windows were quantified and the relative distribution (%) was determined within each lane.

Long 3′ overhangs are highly abundant

In contrast to the situation for *S. cerevisiae* where the 3′ overhangs are hardly distinguishable, the 3′ overhangs were clearly detectable in non-synchronized *S. castellii* cells when analysed by the in-gel hybridization method (Figure 2). This global 3′ overhang signal showed only moderate changes in cells synchronously proceeding from S to G2 phase. To perform a detailed examination of the 3′ overhang lengths, we applied the DSN assay. Astonishingly, this revealed that the 3′ overhangs are as long as 200 nt in *S. castellii*. Moreover, the 3′ overhangs showed a wide size distribution in asynchronous logarithmically growing cells, ranging from 14 to 200 nt in length (Figure 4). Unexpectedly, a large fraction of these 3′ overhangs resides in the 75–200-nt size group. Thus, both the global signal and the length distribution of *S. castellii* 3′ overhangs differ to the situation in *S. cerevisiae*, where the 3′ overhangs are 12–14 nt during most parts of the cell cycle and only extended to >32 nt in late S phase (1,17). It is notable that the observed wide size distribution in *S. castellii* is reminiscent of the 3′ overhang patterns observed for human cells, although the size range is even wider in the human cells (11,16).

The 70-nt 3′ overhangs are generated in S phase

We discovered a remarkably distinct signal of 3′ overhangs with a length of 70 nt. This signal was prominent in samples prepared from cultures with a high cell density ($OD_{600} \geq 0.7$), and after normalization to the amount of probe hybridization, it was still apparent as the most abundant among the sizes present (Figure 5). However, we observed that the amount of 70-nt 3′ overhangs was lower in preparations from cultures with a low cell density. This implied that the generation of 70-nt overhangs is dependent on the status of the cell culture. We believe that our unsynchronized cells may become partially synchronized when reaching a high cell density. Such partial synchronization of cells is a previously recognized feature of yeast cultures [reviewed in (33)]. When reaching a high density, the cells will affect each other, will begin to exhibit a periodic behaviour (oscillation) and will synchronize their growths. This idea of a cell cycle regulated generation of the 70-nt 3′ overhangs was corroborated by our synchronization experiments, where the 70-nt 3′ overhangs became highly abundant during the blocking procedure, whereas they were undetectable in the logarithmically growing cells sampled before the addition of hydroxyurea (Figure 6; 0 versus Pre).

The accumulation of 70-nt-long 3′ overhangs in the cells blocked in S phase was a common and highly robust result for all the synchronization experiments. After release of the cell cycle block in S phase, the signal then gradually diminished during the experimental time course. Although the overall dynamics of the accumulation were highly similar in all experiments, the actual time point for the disappearance of the signal differed somewhat between the experiments (Supplementary Figure S3). Most probably, this was caused by a variation in the time spent for the washing procedure when releasing the cells. When varying the time for the centrifugations, we observed that the cells showed a difference in the extent of progression through S and into G2 phase at the time of release. In an experiment with a longer washing time (Supplementary Figure S4), the cells had advanced further into S than when shorter centrifugations were performed (Supplementary Figure S1A, compare the 0 min time points). Hence, this further supports the conclusion that the 70-nt 3′ overhangs are produced in S phase and then decrease in abundance as the cells proceed to G2. Furthermore, an additional common pattern in all the experiments was the reoccurrence of the 70-nt 3′ overhangs at later time points. This finding can be correlated with the flow cytometry data, which showed that a minor fraction of the cells move in synchrony beyond the G2/M passage. The reoccurrence of the signal coincides with the timing of the next S phase of this cell fraction (Figure 6 and Supplementary Figure S4; 100–120 min). Surprisingly, in the time course experiment lasting for 300 min, we detected weak reappearing signals at three times, thus inferring that the culture kept the synchronous growth to some degree throughout the whole time course (Supplementary Figure S3A). Taken together, the defined length and the restricted timing of their appearance in the cell cycle indicate that the 70 nt 3′ overhangs are generated in the S phase in a highly regulated process. Moreover, we find it noteworthy that a similar defined 3′ overhang signal was observed to appear in the S phase in human cancer cells, although at a size of ~300 nt (11).

Generation of the 70-nt 3′ overhangs is uncoupled to the generation of the bulk of overhangs

The current model for the replication of the telomere in *S. cerevisiae* suggests that a resection of the CA-rich strand takes place to generate the single-stranded 3′ overhang, thus allowing the CST complex (Cdc13–Stn1–Ten1) to bind and recruit telomerase to the 3′-end [reviewed in (4)]. Although the telomerase is responsible for elongating the 3′-end of telomeres, only a small fraction of the telomeres is elongated in every cell cycle (5,6). Instead, a multitude of processes are expected to be involved in the generation of the large pool of 3′ overhangs in the cell. These processes are yet not well defined in terms of timing and extent, and the proteins involved have yet to be identified. For instance, Cdc13

has been shown to interact with the Pol1 subunit of the DNA polymerase α/primase complex, and the CST complex is suggested to be involved in promoting the initiation of the synthesis of the CA-rich strand (34). In fact, the positioning of the replication machinery on the CA-strand, in relation to the 3′-end terminus, may in itself be a factor influencing the resulting 3′ overhang lengths.

Here, we showed that telomerase knock-out cells have a similar wide distribution of 3′ overhang lengths as wild-type cells, inferring that the large pool of 3′ overhangs is generated by various telomerase-independent mechanisms, including resection of the 5′-end. Surprisingly, the distinct class of 70-nt 3′ overhangs is produced specifically in the S phase and is totally lacking in telomerase-deficient cells. Our results thus correlate well with the finding that telomerase action at telomeres is limited to the S phase of the cell cycle (18), and indicate that the 70-nt overhangs are produced by telomerase in a process that is uncoupled to the generation of the bulk 3′ of the overhangs. Our results further imply that the elongation activity of telomerase would be regulated to produce 3′ overhangs with a mean length of ~70 nt (corresponding to ~nine telomeric repeats). In this regard, it is interesting to note that many of the telomere extension events measured in *S. cerevisiae* are within this size range (5,6). Therefore, it would be interesting to further investigate the possible mechanisms for such a regulation. One plausible mechanism would be that the interaction between the polymerase α/primase complex and the CST complex would lead to a termination of the telomerase elongation activity. If this interaction would be performed in a coordinated fashion together with telomerase, it may control and limit the telomerase elongation activity. On the other hand, we could not rule out the possibility that telomerase is instead taking part in the coordination of the replication of the complementary CA-rich strand. Possibly, telomerase could take part in the action to direct the initiation point of the replication to a specific distance upstream from the 3′-end terminus. As for *S. castellii*, this initiation would occur at a distance of 70 nt from the 3′-end, thus leaving a 70-nt-single-stranded stretch before the start of the 5′-end of the complementary CA-strand. In such a scenario, the extension length of the telomerase synthesis could in principle be totally unregulated, as the start of the CA-strand fill-in would here be regulated in relation to a fixed distance from the 3′-end, thus generating well-defined 3′ overhangs at a specific time point in the cell cycle. To further elucidate the molecular mechanism that is responsible for the generation of the specific class of 70-nt 3′ overhangs, it will, therefore, be highly interesting to further pinpoint the exact timing of the appearance of the 70-nt 3′ overhang fraction and to investigate which other factors are involved. In a majority of human tumours, telomere maintenance is essential for the sustained growth of the tumour cells. The unravelling of uncoupled processes and separate regulatory steps within the telomere maintenance will, therefore, provide the possibility to explore new strategies for cancer therapeutics.

SUPPLEMENTARY DATA

Supplementary Data are available at NAR Online: Supplementary Methods and Supplementary Figures 1–4.

ACKNOWLEDGEMENTS

The authors thank Raymund J. Wellinger for valuable advice, and Marie-Louice Kristensson and Martina Gsell for technical assistance. They are grateful to Yong Zhao and Woodring E. Wright for advice regarding the DSN assay, and Stina Oredsson for help with the flow cytometry analyses.

FUNDING

Carl Trygger Foundation; Royal Physiographic Society in Lund; Jörgen Lindström Foundation; Swedish Research Council; Sven and Lilly Lawski Foundation scholarship (to E.A.). Funding for open access charge: Swedish Government.

Conflict of interest statement. None declared.

REFERENCES

1. Wellinger,R.J., Wolf,A.J. and Zakian,V.A. (1993) *Saccharomyces* telomeres acquire single-strand TG1-3 tails late in S phase. *Cell*, **72**, 51–60.
2. Wellinger,R.J., Ethier,K., Labrecque,P. and Zakian,V.A. (1996) Evidence for a new step in telomere maintenance. *Cell*, **85**, 423–433.
3. Makarov,V.L., Hirose,Y. and Langmore,J.P. (1997) Long G tails at both ends of human chromosomes suggest a C strand degradation mechanism for telomere shortening. *Cell*, **88**, 657–666.
4. Shore,D. and Bianchi,A. (2009) Telomere length regulation: coupling DNA end processing to feedback regulation of telomerase. *EMBO J.*, **28**, 2309–2322.
5. Teixeira,M.T., Arneric,M., Sperisen,P. and Lingner,J. (2004) Telomere length homeostasis is achieved via a switch between telomerase- extendible and -nonextendible states. *Cell*, **117**, 323–335.
6. Chang,M., Arneric,M. and Lingner,J. (2007) Telomerase repeat addition processivity is increased at critically short telomeres in a Tel1-dependent manner in *Saccharomyces cerevisiae*. *Genes Dev.*, **21**, 2485–2494.
7. Tseng,S.F., Lin,J.J. and Teng,S.C. (2006) The telomerase-recruitment domain of the telomere binding protein Cdc13 is regulated by Mec1p/Tel1p-dependent phosphorylation. *Nucleic Acids Res.*, **34**, 6327–6336.
8. Tseng,S.F., Shen,Z.J., Tsai,H.J., Lin,Y.H. and Teng,S.C. (2009) Rapid Cdc13 turnover and telomere length homeostasis are controlled by Cdk1-mediated phosphorylation of Cdc13. *Nucleic Acids Res.*, **37**, 3602–3611.
9. Li,S., Makovets,S., Matsuguchi,T., Blethrow,J.D., Shokat,K.M. and Blackburn,E.H. (2009) Cdk1-dependent phosphorylation of Cdc13 coordinates telomere elongation during cell-cycle progression. *Cell*, **136**, 50–61.
10. Lingner,J., Cooper,J.P. and Cech,T.R. (1995) Telomerase and DNA end replication: no longer a lagging strand problem? *Science*, **269**, 1533–1534.
11. Zhao,Y., Sfeir,A.J., Zou,Y., Buseman,C.M., Chow,T.T., Shay,J.W. and Wright,W.E. (2009) Telomere extension occurs at most chromosome ends and is uncoupled from fill-in in human cancer cells. *Cell*, **138**, 463–475.
12. Bonetti,D., Martina,M., Clerici,M., Lucchini,G. and Longhese,M.P. (2009) Multiple pathways regulate 3′ overhang generation at *S. cerevisiae* telomeres. *Mol. Cell*, **35**, 70–81.

13. Sfeir,A.J., Shay,J.W. and Wright,W.E. (2005) Fine-tuning the chromosome ends: the last base of human telomeres. *Cell Cycle*, **4**, 1467–1470.
14. Suzuki,T., McKenzie,M., Ott,E., Ilkun,O. and Horvath,M.P. (2006) DNA binding affinity and sequence permutation preference of the telomere protein from *Euplotes crassus*. *Biochemistry*, **45**, 8628–8638.
15. Loayza,D. and De Lange,T. (2003) POT1 as a terminal transducer of TRF1 telomere length control. *Nature*, **424**, 1013–1018.
16. Zhao,Y., Hoshiyama,H., Shay,J.W. and Wright,W.E. (2008) Quantitative telomeric overhang determination using a double-strand specific nuclease. *Nucleic Acids Res.*, **36**, e14.
17. Larrivee,M., LeBel,C. and Wellinger,R.J. (2004) The generation of proper constitutive G-tails on yeast telomeres is dependent on the MRX complex. *Genes Dev.*, **18**, 1391–1396.
18. Marcand,S., Brevet,V., Mann,C. and Gilson,E. (2000) Cell cycle restriction of telomere elongation. *Curr. Biol.*, **10**, 487–490.
19. Taggart,A.K., Teng,S.C. and Zakian,V.A. (2002) Est1p as a cell cycle-regulated activator of telomere-bound telomerase. *Science*, **297**, 1023–1026.
20. Cliften,P.F., Fulton,R.S., Wilson,R.K. and Johnston,M. (2006) After the duplication: gene loss and adaptation in *Saccharomyces* genomes. *Genetics*, **172**, 863–872.
21. Gordon,J.L., Armisen,D., Proux-Wera,E., OhEigeartaigh,S.S., Byrne,K.P. and Wolfe,K.H. (2011) Evolutionary erosion of yeast sex chromosomes by mating-type switching accidents. *Proc. Natl Acad. Sci. USA*, **108**, 20024–20029.
22. Astromskas,E. and Cohn,M. (2007) Tools and methods for genetic analysis of *Saccharomyces castellii*. *Yeast*, **24**, 499–509.
23. Astromskas,E. and Cohn,M. (2009) Ends-in vs. ends-out targeted insertion mutagenesis in *Saccharomyces castellii*. *Curr. Genet.*, **55**, 339–347.
24. Cohn,M. and Blackburn,E.H. (1995) Telomerase in yeast. *Science*, **269**, 396–400.
25. Cohn,M., McEachern,M.J. and Blackburn,E.H. (1998) Telomeric sequence diversity within the genus *Saccharomyces*. *Curr. Genet.*, **33**, 83–91.
26. Wahlin,J. and Cohn,M. (2002) Analysis of the RAP1 protein binding to homogeneous telomeric repeats in *Saccharomyces castellii*. *Yeast*, **19**, 241–256.
27. Rhodin,J., Astromskas,E. and Cohn,M. (2006) Characterization of the DNA binding features of *Saccharomyces castellii* Cdc13p. *J. Mol. Biol.*, **355**, 335–346.
28. Rhodin Edsö,J., Tati,R. and Cohn,M. (2008) Highly sequence-specific binding is retained within the DNA-binding domain of the *Saccharomyces castellii* Cdc13 telomere-binding protein. *FEMS Yeast Res.*, **8**, 1289–1302.
29. Rhodin Edsö,J., Gustafsson,C. and Cohn,M. (2011) Single- and double-stranded DNA binding proteins act in concert to conserve a telomeric DNA core sequence. *Genome Integr.*, **2**, 2.
30. Philippsen,P., Stotz,A. and Scherf,C. (1991) DNA of *Saccharomyces cerevisiae*. *Methods Enzymol.*, **194**, 169–182.
31. Dionne,I. and Wellinger,R.J. (1996) Cell cycle-regulated generation of single-stranded G-rich DNA in the absence of telomerase. *Proc. Natl Acad. Sci. USA*, **93**, 13902–13907.
32. Amon,A. (2002) Synchronization procedures. *Methods Enzymol.*, **351**, 457–467.
33. Richard,P. (2003) The rhythm of yeast. *FEMS Microbiol. Rev.*, **27**, 547–557.
34. Qi,H. and Zakian,V.A. (2000) The *Saccharomyces* telomere-binding protein Cdc13p interacts with both the catalytic subunit of DNA polymerase alpha and the telomerase-associated est1 protein. *Genes Dev.*, **14**, 1777–1788.